First-principles study of orbital ordering in cubic fluoride $KCrF_3$*

Ming Xing(明 星)[a)b)], Xiong Liang-Bin(熊良斌)[a)], Xu Huo-Xi(徐火希)[a)],
Du Fei(杜 菲)[b)], Wang Chun-Zhong(王春忠)[b)], and Chen Gang(陈 岗)[b)†]

[a)] *College of Physics and Electronic Information, Huanggang Normal University, Huanggang* 438000, *China*
[b)] *College of Physics, State Key Laboratory of Superhard Materials, Jilin University, Changchun* 130012, *China*

(Received 14 June 2013; revised manuscript received 3 September 2013; published online 24 January 2014)

Comprehensive first-principles calculations are performed to provide insight into the intriguing physical properties of the ternary cubic fluoride $KCrF_3$. The electronic structures exhibit a prominent dependence on the effective local Coulomb interaction parameter $U_{\rm eff}$. The ground state of the cubic phase is a ferromagnetic (FM) half-metal with $U_{\rm eff}$ equal to 0, 2, and 4 eV, whereas the insulating A-type antiferromagnetic (A-AFM) state with concomitant homogeneous orbital ordering is more robust than the FM state for $U_{\rm eff}$ exceeding 4 eV. We propose that the origin of the orbital ordering is purely electronic when the cooperative Jahn–Teller distortions are absent in cubic $KCrF_3$.

Keywords: electron density of states, band structure, orbital ordering, first-principles calculations

PACS: 74.25.Ha, 71.20.Be, 71.15.Mb **DOI:** 10.1088/1674-1056/23/3/037401

1. Introduction

Due to the interplay between charge, spin, orbital and lattice degrees of freedom, transition-metal oxides exhibit profuse and exotic structural, electronic, and magnetic properties, which are at the forefront of contemporary multidisciplinary.[1,2] Especially, perovskite compounds have attracted considerable attention due to the Jahn–Teller (JT) active ions (for example, Mn^{3+} (d^4) and Cu^{2+} (d^9) ions) and active orbital degrees of freedom.[3] For instance, the parent compound of the fascinating colossal magnetoresistance effect, manganite $LaMnO_3$,[4] and the model compound of one-dimensional (1D) $S = 1/2$ Heisenberg antiferromagnet, pseudocubic cuprate $KCuF_3$, have long been known as the prototype materials for cooperative JT distortion (CJTD) and orbital ordering.[5]

In recent years, renewed attention has been paid to the topics of orbital ordering and the interactions between charge, orbital, and magnetic ordering in correlated electronic systems. Curiously, most of the research interests have focused almost exclusively on oxides. Similar intriguing electronic and magnetic phenomena should also exist in other families of correlated systems, such as sulfides, nitrides, and fluorides. The ternary fluoride $KCrF_3$ has remarkable similarities to both $LaMnO_3$ and $KCuF_3$. $KCrF_3$ crystallizes in a perovskite-type structure at ambient condition and it contains the JT active ion of Cr^{2+} (d^4). Edwards *et al.*[6] first reported that $KCrF_3$ adopted a tetragonal structure at room temperature (space group $P4/mmm$). Powder neutron diffraction experiments[7] showed a magnetic transition to the A-type antiferromagnetic (A-AFM) structure at $T_{\rm N} = 40$ K.

Recently, the structural and magnetic properties of $KCrF_3$ have been reinvestigated by high-resolution synchrotron X-ray powder diffraction and neutron powder-diffraction methods.[8,9] $KCrF_3$ displays three different crystallographic structures. At very high temperatures, $KCrF_3$ adopts an idea cubic perovskite structure with space group $Pm\text{-}3m$.[8,9] Below 973 K, it adopts a body-centered tetragonal structure (space group $I4/mcm$) and exhibits a strong CJTD, which indicates the presence of an antiferrodistortive orbital ordering. Below 250 K, $KCrF_3$ undergoes a phase transition to a more complicated monoclinic structure with space group $I2/m$. Magnetic measurement showed that $KCrF_3$ possesses long-range AFM ordering below the magnetic transition temperature of 46 K.[8,9]

The high-temperature tetragonal and low-temperature monoclinic phases of $KCrF_3$ have been systematically investigated by Xu *et al.*[10] They employed the full-potential linearized augmented plane wave plus local orbital (FP-LAPW + LO) method within the generalized gradient approximation (GGA) and the local spin density approximation plus on-site Coulomb repulsion (LSDA + U) approach. The electronic, magnetic, and orbital structures of $KCrF_3$ are also investigated for all three crystallographic phases (cubic, tetragonal, and monoclinic) by Giovannetti *et al.* within *ab initio* LSDA and LSDA + U calculations.[11] Their calculated results revealed that the ground state is A-AFM Mott insulators for both tetragonal and monoclinic phases, which exhibits CJTD concomitant with staggered G-type orbital ordering. Giovannetti *et al.*[11] considered A-AFM and C-AFM magnetic ordering states of the high-temperature cubic phase. They pointed out

*Project supported by the National Natural Science Foundation of China (Grant Nos. 11104101 and 11004073) and the Scientific and Technologic Research Program of Department of Education of Hubei Province, China (Grant No. D20132902).

†Corresponding author. E-mail: mingxing06@mails.jlu.edu.cn

© 2014 Chinese Physical Society and IOP Publishing Ltd

that the electronic structure of cubic $KCrF_3$ displays a dependence on the exchange-correlation (XC) functions. The cubic phase appears as a metal from LSDA, but it becomes a Mott insulator concomitant homogeneous orbital orderings at the LSDA + U level. Recently, the electronic, magnetic, and orbital structures of $KCrF_3$ were studied by performing first-principles calculations within both GGA and GGA + U in the tetragonal and cubic phases.[12–14] They claimed that the electron–electron interactions rather than the electron–phonon interactions were the driving forces behind the orbital ordering in $KCrF_3$.

In this paper, we carry out first-principles electronic structure calculations to gain insight into the intriguing physical properties of the cubic $KCrF_3$. The dependence of the ground-state electronic structure on the effective local Coulomb interaction parameter $U_{\rm eff}$ ($U_{\rm eff} = U - J$), and the origin of the orbital ordering are studied and discussed by comprehensive density functional calculations. The theoretical investigations provide further details for better understanding of the ternary transition-metal fluoride $KCrF_3$.

2. Computational details

The *ab initio* calculations are performed within the plane-wave pseudopotential method encoded in the CASTEP code[15] based on density functional theory (DFT). The exchange–correlation potential is handled within the spin-polarized GGA in the Perdew–Burke–Ernzerhof (PBE) scheme.[16] To account for the strong Coulomb repulsion and exchange interaction of the partial filled Cr 3d electrons, we adopt the GGA+U (U denotes on-site coulomb repulsion) approach proposed by Dudarev *et al.*[17,18] to incorporate the on-site Coulomb repulsion U and exchange interaction J into the density functional. The applied GGA + U approach has the advantage that only one unknown parameter $U_{\rm eff}$ ($U_{\rm eff} = U - J$) needs to be introduced. After careful convergence testing, the plane-wave cutoff energy is set to be 700 eV and requested k-point spacing is fixed to be 0.04 Å^{-1} for all calculations.

The initial crystal structure model of cubic $KCrF_3$ is built according to the experimental crystal structure parameters as reported in Ref. [9]. Here we consider four possible magnetic configurations to explore the electronic structure and magnetic properties of cubic $KCrF_3$. Calculations are performed for the ferromagnetic (FM) and three different kinds of AFM spin ordering states, which are constructed as follows. All spins are parallel aligned in the FM state for a primitive cell, FM *ab* planes are stacked antiferromagnetically along the c direction in A-AFM state for a $1\times1\times2$ supercell, AFM *ab* planes are stacked ferromagnetically along the c direction in C-AFM state for a $\sqrt{2}\times\sqrt{2}\times1$ supercell, and the AFM is along all three directions in G-AFM state for a $2\times2\times2$ supercell.

3. Results and discussion

We first calculate the total energies and magnetic moments for considered magnetic configurations with the GGA scheme, and then proceed to include local correlations within the GGA+U approach. The GGA+U method is known to improve over GGA in strong correlated transition-metal systems, but a suitable choice of the parameters is not possible at present because sufficient experimental information is not available for cubic $KCrF_3$. We perform calculations for a series of values of the Coulomb parameter $U_{\rm eff}$ ($U_{\rm eff} = U - J$), namely, $U_{\rm eff}$ is equal to 2, 4, 6, 8, and 10 eV.

The differences in energies between various magnetic ordering states are reported in Table 1. It can be seen that the total energy of the FM state is the lowest among all four considered magnetic configurations, which is the most stable solution in the viewpoint of energy. The calculated magnetic moment is close to $4\mu_{\rm B}$ per Cr atom, which implies a high-spin configuration in accordance with Hund's rule.

Table 1. Calculated total energies for the four spin configurations of cubic $KCrF_3$ by means of the GGA+U approach with different $U_{\rm eff}$ values. All the energies (in units of meV/f.u.) are given relative to that of the FM state.

$U_{\rm eff}$/eV	A-AFM	C-AFM	G-AFM
0	88.5	206.7	333.9
2	99.2	225.4	231.7
4	25.6	57.1	49.9
6	1.8	19.0	16.2
8	3.8	13.9	14.6
10	6.2	12.2	15.8

The spin-polarized band structure of cubic $KCrF_3$ for the FM state within GGA calculations is shown in Fig. 1. The exchange splitting is very large, which moves the minority-spin bands far above the Fermi level. The Cr 3d levels are split into three-fold degenerate t_{2g} (d_{xy}, d_{yz}, d_{zx}) and doubly degenerate e_g (d_{z^2}, $d_{x^2-y^2}$) levels in the octahedral crystal field. The JT distortion has been removed in the cubic phase, and the e_g band is half-filled even though it is fully spin polarized. The Fermi energy cuts through the majority-spin Cr 3d states, whereas the minority-spin channel forms an insulating gap, which displays a prominent characteristic of the half-metallic ferromagnet.[19]

To properly describe the strong electron correlation of Cr 3d electrons in cubic $KCrF_3$, we employ the GGA+U method. Calculated results indicate that the qualitative characteristics of the electronic structure for the FM state have not changed from $U_{\rm eff} = 2$ to 4 eV, whereas it appears as an FM insulator when $U_{\rm eff}$ exceeds 4 eV. As shown in Fig. 2, an insulating gap of 0.7 eV opens up in the majority-spin Cr e_g state ($U_{\rm eff} = 6$ eV). Along with the increase in $U_{\rm eff}$, the band gap is further enlarged from 1.57 eV ($U_{\rm eff} = 8$ eV) to 2.43 eV ($U_{\rm eff} = 10$ eV). As expected, the GGA+U approach tends to enhance the localization of Cr 3d states and push unoccupied

states to higher energy region, thereby increasing the band gap.[10]

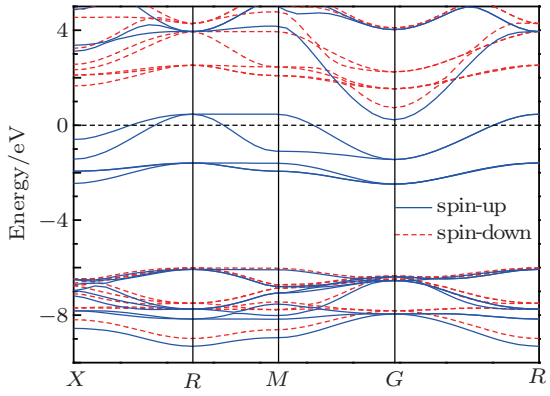


Fig. 1. (color online) Band structure of cubic $KCrF_3$ for the FM spin configuration within the GGA calculations. The spin-up/down subbands are plotted with solid/dashed lines, respectively. Fermi level (E_F) is set to 0 eV.

In fact, the energy of the A-AFM state is comparable to the FM state when U_{eff} exceeds 4 eV (as shown in Table 1). Such a small difference may place in the calculation error, and the real state adopted by the material is not determined by the energy any more.[20] Giovannetti *et al.* claimed that cubic $KCrF_3$ is metallic for the A-AFM magnetic structure at the LSDA level, whereas a band gap of 1.72 eV opens up with the LSDA + U method ($U = 6.0$ and $J = 0.88$ eV).[11] Figure 3 displays the band structure of the A-AFM state, which confirms that the cubic $KCrF_3$ is an insulator with a band gap of 1.6 eV ($U_{eff} = 6$ eV).

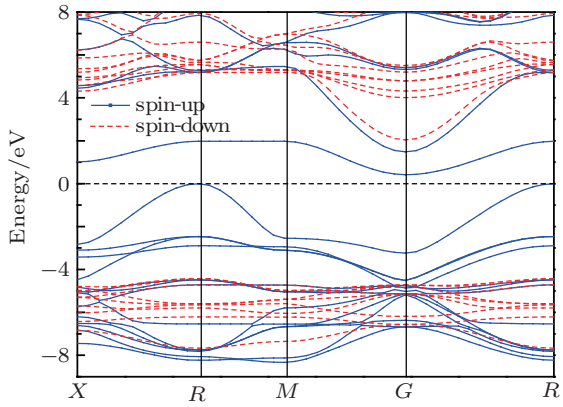


Fig. 2. (color online) Band structure of cubic $KCrF_3$ for the FM spin configuration within the GGA+U approach ($U_{eff} = 6$ eV).

The Jahn–Teller distortions are absent in high-temperature cubic $KCrF_3$ consisting of equivalent Cr–F bond lengths and regular CrF_6 octahedra. Normally, the 3d levels should split into three-fold degenerate t_{2g} and doubly degenerate e_g levels in the octahedral crystal field. However, the degeneracy of the e_g level can be further lifted by the on-site Coulomb repulsion interactions. The e_g levels are split into one fully occupied d_{z^2} orbital and another nearly unoccupied $d_{x^2-y^2}$ orbital. An energy gap opens up between the occupied and unoccupied bands. An orbital ordering appears, as shown in Fig. 4. For the two nearly degenerate FM and A-AFM spin ordering states, we obtain a homogeneous orbital occupation of d_{z^2} orienting perpendicular to the FM *ab* plane. The motifs of orbital ordering in the present work are essentially identical to those in Ref. [11] (see Fig. 9 in Ref. [11]).

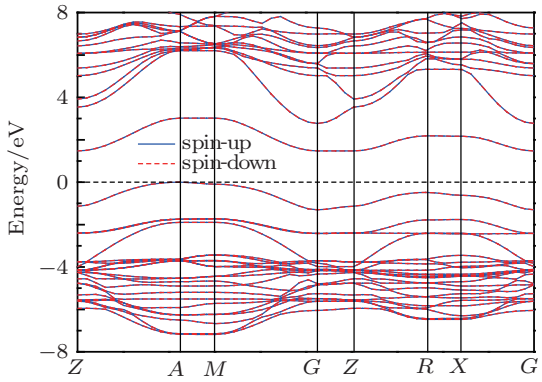


Fig. 3. (color online) Band structure of cubic $KCrF_3$ for the A-AFM spin configuration within the GGA+U approach (U_{eff} = 6 eV). The prominent characteristic is that the spin-up and spin-down subbands are overlapped to each other, displaying the unique characteristic of the AFM ordering.

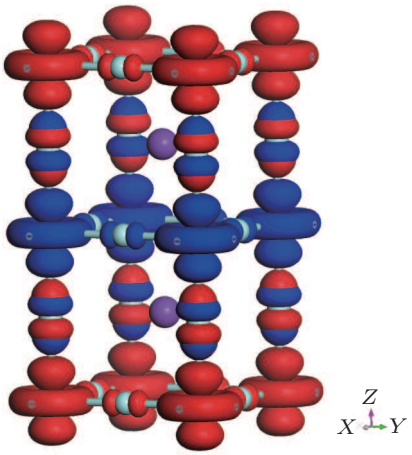


Fig. 4. (color online) Spin density plot corresponding to the occupied e_g bands from the result of GGA+U (U_{eff} = 6 eV) calculations for the A-AFM state.

Calculated electronic structures suggest that the on-site Coulomb repulsion in $KCrF_3$ plays an important role in forming the orbital ordering. There are two mechanisms of orbital ordering: the lattice instability of one-electron electron–phonon coupling[5,21,22] and a purely electronic mechanism of many-body Kugel–Khomskii (KK) super-exchange.[5,23] For a pair of Cr^{3+} ions, hopping only occurs between two d_{z^2} orbitals, hopping between d_{z^2} and $d_{x^2-y^2}$ orbitals is zero by symmetry, and the overlap between two $d_{x^2-y^2}$ orbitals in the z direction is very small.[24] According to the Goodenough–Kanamori–Anderson (GKA) rules, the overlap of single filled d_{z^2} orbitals leads to a strong AFM exchange interaction in the

c direction, whereas the overlap of a filled d_{z^2} orbital and an empty $d_{x^2-y^2}$ orbital gives rise to an FM coupling in the ab plane. The insulating A-AFM state of the cubic phase with concomitant homogeneous orbital ordering is more robust than the FM state, which is reminiscent of the cases in $LaMnO_3$ and $KCuF_3$,[25] where the orbital ordering in both compounds is purely electronic in origin.

The orbital ordering in high-temperature cubic $KCrF_3$ is interesting from a theoretical perspective. However, the presence of long-range magnetic ordering at high temperatures for the cubic phase is impossible.[11] It is reasonable to suppose the presence of orbital ordering in high-temperature cubic paramagnetic (PM) $KCrF_3$.[25] Therefore, high-temperature magnetic measurement will be invaluable to explore the exact nature of magnetic configurations in the cubic phase. Complementary heat capacity and resistivity measurements would also be fundamental to clarify the essence of the orbital ordering (or disordering) state.

4. Conclusions

We have performed first-principles electronic structure calculations on the cubic $KCrF_3$ by considering one FM and three different typical AFM (A-AFM, C-AFM and G-AFM) configurations. Calculated results demonstrate that the ground-state electronic structures exhibit a prominent dependence on the effective local Coulomb interaction parameter U_{eff}. The ground state of the cubic phase is an FM half-metal with U_{eff} values equal to 0, 2, and 4 eV, whereas the insulating A-AFM state with concomitant homogeneous orbital ordering is more robust than the FM state for U_{eff} exceeding 4 eV. We suggest that the orbital ordering in cubic $KCrF_3$ is purely electronic in origin.

References

[1] Tokura Y and Nagaosa N 2000 *Science* **288** 462
[2] Jiang Q, Kang Y T and Yao D X 2013 *Chin. Phys. B* **22** 087402
[3] Imada M, Fujimori A and Tokura Y 1998 *Rev. Mod. Phys.* **70** 1039
[4] Bao J C, Zhang N, Cao H X and Geng T 2008 *Chin. Phys. B* **17** 317
[5] Liu D Y, Chen D M and Zou L J 2009 *Chin. Phys. B* **18** 4497
[6] Edwards A J and Peacock R D 1959 *J. Chem. Soc.* **41** 26
[7] Yoneyama S and Hirakawa K 1966 *J. Phys. Soc. Jpn.* **21** 183
[8] Margadonna S and Karotsis G 2006 *J. Am. Chem. Soc.* **128** 16436
[9] Xiao Y, Su Y, Li H F, Kumar C M N, Mittal R, Persson J, Senyshyn A, Gross K and Brueckel Th 2010 *Phys. Rev. B* **82** 094437
[10] Xu Y H, Hao X F, Lü M F, Wu Z J, Zhou D F and Meng J 2008 *J. Chem. Phys.* **128** 164721
[11] Giovannetti G, Margadonna S and van den Brink J 2008 *Phys. Rev. B* **77** 075113
[12] Wang G T, Li Z, Zheng L H and Yang Z X 2011 *Phys. Rev. B* **84** 045111
[13] Wang G T, Zhang M P, Li Z and Zheng L H 2012 *Acta Phys. Sin.* **61** 37102 (in Chinese)
[14] Zhang M P and Wang G T 2012 *Mod. Phys. Lett. B* **26** 1150025
[15] Segall M D, Lindan P J D, Probert M J, Pickard C J, Hasnip P J, Clark S J and Payne M C 2002 *J. Phys.: Condens. Matter* **14** 2717
[16] Perdew J P, Burke K and Ernzerhof M 1996 *Phys. Rev. Lett.* **77** 3865
[17] Dudarev S L, Botton G A, Savrasov S Y, Humphreys C J and Sutton A P 1998 *Phys. Rev. B* **57** 1505
[18] Cococcioni M and de Gironcoli S 2005 *Phys. Rev. B* **71** 035105
[19] de Groot R A, Mueller F M, van Engen P G and Buschow K H J 1983 *Phys. Rev. Lett.* **50** 2024
[20] Huang Z F, Du F, Wang C Z, Wang D P and Chen G 2007 *Phys. Rev. B* **75** 054411
[21] Gehring G A and Gehring K A 1975 *Rep. Prog. Phys.* **38** 1
[22] Engleman R and Halperin B 1970 *Phys. Rev. B* **2** 75
[23] Kugel K I and Khomskii D I 1973 *Sov. Phys. JETP* **37** 725
[24] Khomskii D I and Mostovoy M V 2003 *J. Phys. A: Math. Gen.* **36** 9197
[25] Medvedeva J E, Korotin M A, Anisimov V I and Freeman A J 2002 *Phys. Rev. B* **65** 172413